Surgery 166 (2019) 991–996

Contents lists available at ScienceDirect

Surgery

journal homepage: www.elsevier.com/locate/surg

Pancreas

Prevention of early liver metastasis after pancreatectomy by perioperative administration of a nuclear factor-κB inhibitor in mice

Nobuhiro Saito, MD, PhD[a,b,*], Tadashi Uwagawa, MD, PhD, FACS[a,c], Ryouga Hamura, MD[a,b], Naoki Takada, MD[a,b], Hiroshi Sugano, MD, PhD[a,b], Yoshihiro Shirai, MD, PhD[a,b], Hiroaki Shiba, MD, PhD[a], Toya Ohashi, MD, PhD[b], Katsuhiko Yanaga, MD, PhD, FACS[a]

[a] Department of Surgery, Jikei University School of Medicine, Tokyo, Japan
[b] Division of Gene Therapy, Research Center for Medical Science, Jikei University School of Medicine, Tokyo, Japan
[c] Division of Clinical Oncology and Hematology, Department of Internal Medicine, Jikei University School of Medicine, Tokyo, Japan

ARTICLE INFO

Article history:
Accepted 27 May 2019
Available online 26 July 2019

ABSTRACT

Background: Liver metastasis is a common problem after pancreatectomy for pancreatic cancer. In pancreatic cancer cells, nuclear factor-κB is activated constitutively. Nuclear factor-κB activates matrix metalloproteinase-2/9, which plays an important role in cancer metastasis. Because the serine protease inhibitor FUT-175 suppresses nuclear factor-κB, we hypothesized that perioperative treatment with FUT-175 for pancreatic cancer may help to prevent liver metastasis.

Methods: We compared in vitro cell viability, cell invasiveness, nuclear factor-κB signaling, and the expression levels of matrix metalloproteinase signals between the control group (C group) and the FUT-175 group (F group) using the murine pancreatic cancer cells PAN02. In addition, we evaluated the in vivo effect of pretreatment with FUT-175 using an established model of liver metastasis in mice. Metastatic liver lesions were assessed with magnetic resonance imaging. Liver recurrence and overall survival were evaluated. Also, the antimetastatic effect of systemic administration of FUT-175 was examined.

Results: FUT-175 did not suppress the cell viability of PAN02 cells at or after 24 hours of treatment ($P > .05$); however, cell invasion was suppressed in the F group compared with the C group ($P < .05$). The levels of nuclear factor-κB activation, membrane type-1 (MT-1) matrix metalloproteinase (MMP)/matrix metalloproteinase-14 (MMP-14), and matrix metalloproteinase-2/9 (MMP-2/9) were lower in the F group compared with the C group. In vivo, both disease-free and overall survivals were prolonged in the F group compared with the C group. Systemic administration was also effective in suppressing the number of metastases.

Conclusion: Perioperative treatment with FUT-175 may help to prevent early liver metastasis after pancreatectomy for pancreatic cancer.

Introduction

Pancreatic cancer is the fourth leading cause of cancer-related death in developed countries.[1] Even if pancreatic cancers are resected early, further recurrence in the liver is common. Importantly, nuclear factor-κB (NF-κB) is activated constitutively in most pancreatic cancer cells. The NF-κB pathway seems to play a very important role in cancer metastasis.[2] NF-κB upregulates matrix metalloproteinase (MMP)-2/9,[3,4] intracellular adhesion molecule (ICAM),[5] and vascular endothelial growth factor (VEGF).[6] Degradation of the basement membrane by MMP-2/9 leads tumor cells to be able to infiltrate into various organs.[7–10] As we have shown in a previous study, the serine proteinase

Nobuhiro Saito contributed to conceptualization, project administration, data curation, formal analysis, investigation, methodology, and in writing the original draft. Tadashi Uwagawa and Katsuhiko Yanaga contributed to conceptualization, project administration, review, and editing. Ryouga Hamura and Naoki Takada contributed to the formal analysis, investigation, and methodology. Hiroshi Sugano contributed to data curation, formal analysis, investigation, methodology, review, and editing. Yoshihiro Shirai and Hiroaki Shiba contributed to conceptualization, review, and editing. Toya Ohashi contributed to project administration.

* Reprint requests: Nobuhiro Saito, Department of Surgery, Jikei University School of Medicine, 3-25-8, Nishi-shinbashi, Minato-ku, Tokyo 105-8461, Japan.
E-mail address: h24dr-saito@jikei.ac.jp (N. Saito).

https://doi.org/10.1016/j.surg.2019.05.044

inhibitor nafamostat mesilate (FUT-175) decreases the activation levels of MMP-9 and ICAM by suppressing the NF-κB pathway.[11] We hypothesized that perioperative administration of FUT-175 for pancreatic cancer may help to inhibit early liver metastasis and improve postoperative survival.

Materials and Methods

Cell culture

The murine pancreatic cancer cell line PAN02, purchased from the National Cancer Institute (Frederick, MD), was maintained in Roswell Park Memorial Institute (RPMI) medium-1640 (Wako Pure Chemical Industries, Ltd, Osaka, Japan) containing 10% fetal bovine serum (Gibco, Grand Island, NY) and 1% penicillin/streptomycin (Pen Strep, Gibco). The cells were cultured at 37°C with 5% CO_2.

Reagents

FUT-175 was purchased from Torii Pharmaceutical Co, Ltd (Tokyo, Japan) and was dissolved in distilled water and stored at −20°C until use.

Antibodies

Monoclonal antibodies to the inhibitor of κBα (IκBα), phosphorylated IκBα, NF-κB (p65), MMP-2/9, and CD54 (ICAM-1) were purchased from Cell Signaling Technology (Beverly, MA). Anti−β-actin antibody was purchased from Sigma-Aldrich (St. Louis, MO). Monoclonal antibody against VEGF (A-20) was purchased from Santa Cruz Biotechnology, Inc (Santa Cruz, CA). Anti−MMP-14 antibody was purchased from abcam PLC (Cambridge, UK).

Animals

Seven-week-old male mice (C57BL/6JJcl) purchased from CLEA Japan, Inc (Tokyo, Japan) were housed under specific pathogen−free conditions in a biologic cabinet at the Laboratory Animal Facility of the Jikei University School of Medicine. The protocol for the animal experiments was approved by the institutional animal care and use committee of the Jikei University (no. 2017-031) and adhered to the guidance set forth in the *Guidelines for the Proper Conduct of Animal Experiments*, published by the Science Council of Japan in 2006. All the protocols are based on the Declaration of Helsinki.

In vitro experimental protocol

PAN02 cells were treated in 2 conditions: FUT-175 (80 μg/mL) as the treatment group (F group) and vehicle only (distilled water) as the control group (C group) for the appropriate time in each analysis. The concentration of FUT-175 was determined according to previous studies.[12,13]

In vivo experimental animal model and protocol

A well-characterized model of liver metastasis in mice was used.[14] The mice were anesthetized continuously with 2% isoflurane (Pfizer Japan, Tokyo, Japan), and a 5-mm incision was made in the left flank on the splenic silhouette. PAN02 cells (1×10^6 cells) pretreated with FUT-175 (F group) for 24 h or with vehicle only (C group) were suspended in 40 μL of phosphate-buffered saline and injected into the spleen ($n = 10$ for each group). After injection, the abdominal wound was closed in 2 layers. Liver metastases were evaluated sequentially once a week by magnetic resonance imaging (MRI). When the general condition of the mouse reached the criteria described below, they were killed within 24 h, and the liver tumors were evaluated by various assays.

Effects of systemic administration of FUT-175 on liver metastasis

The experiment above is an experiment by pretreatment. Meanwhile, the effects of systemic administration were also examined. 1×10^6 PAN02 cells suspended in 40 μL of phosphate-buffered saline were injected into the spleen of mice ($n = 10$ each for the C and F groups). For the F group, FUT-175 was administrated intraperitoneally at 30 mg/kg 3 times a week starting the day after the operation. Because esterase activity is strong in mice and intravenous injection is not desirable, intraperitoneal administration was used.[15] For the C group, 0.9% NaCl was administered intraperitoneally in the same schedules as in the F group. Seven days later, the mice were killed and the number of metastatic liver nodules counted. The observation period was determined with reference to the disease-free survival (DFS) in the original experiment.

Criteria for killing the animals either before or at the end of the experiment

The animals were killed when they either reached the established criteria or if they become unwell. Mice were killed before the planned end of the experiment if they fulfilled the following conditions: (1) The mouse could not eat or drink for 24 to 48 hours;[16] (2) the mouse lost 20% of their body weight or maintained a body weight loss of 15% for 72 hours compared with age-matched controls[16]; and (3) the mouse developed marked abdominal distention or the ascites burden exceeded an estimated 10% of the body weight of age-matched controls.[16,17]

Cell proliferation assay

The cells were seeded into 96-well plates (5×10^3 cells/well) treated with FUT-175 (80 μg/mL) for 48 hours. The cell proliferation was measured using a CellTiter-Blue Cell Viability Assay Kit (Promega, Madison, WI), according to the manufacturer's instructions. The stained cells were analyzed with a Perkin Elmer EnSpire plate reader (Perkin Elmer, Inc, Waltham, MA).

Invasion assay

PAN02 cells (5×10^6) were seeded into a 6-cm dish. After the cells had reached 90% confluence in 3 days, they were treated with FUT-175 (F group) or with vehicle alone (C group) for 24 hours. Controlled scratches 10 mm in width were made in each dish, and the media were changed to a serum-free medium. Changes in the width of the scratch were observed at 0, 24, and 48 hours after the scratch was made.

Western blotting

PAN02 cells (1×10^6) were seeded into a 6-cm dish. After a 24-hour incubation, the cells were treated with FUT-175 (80 μg/mL) as the F group or treated with vehicle alone (distilled water) as the C group for 24 hours. Whole-protein extracts from both in vitro and in vivo experiments were prepared according to the protocol described previously.[18] The lysate protein was extracted by 2% sodium dodecyl sulfate, electrophoresed on 4% to 20% acrylamide gradient gels in Tris-glycine buffer, and transferred onto a nitrocellulose membrane. After incubating the blots with each primary antibody (IκBα, phosphorylated IκBα, NF-κB [p65], MMP-2/9, CD54

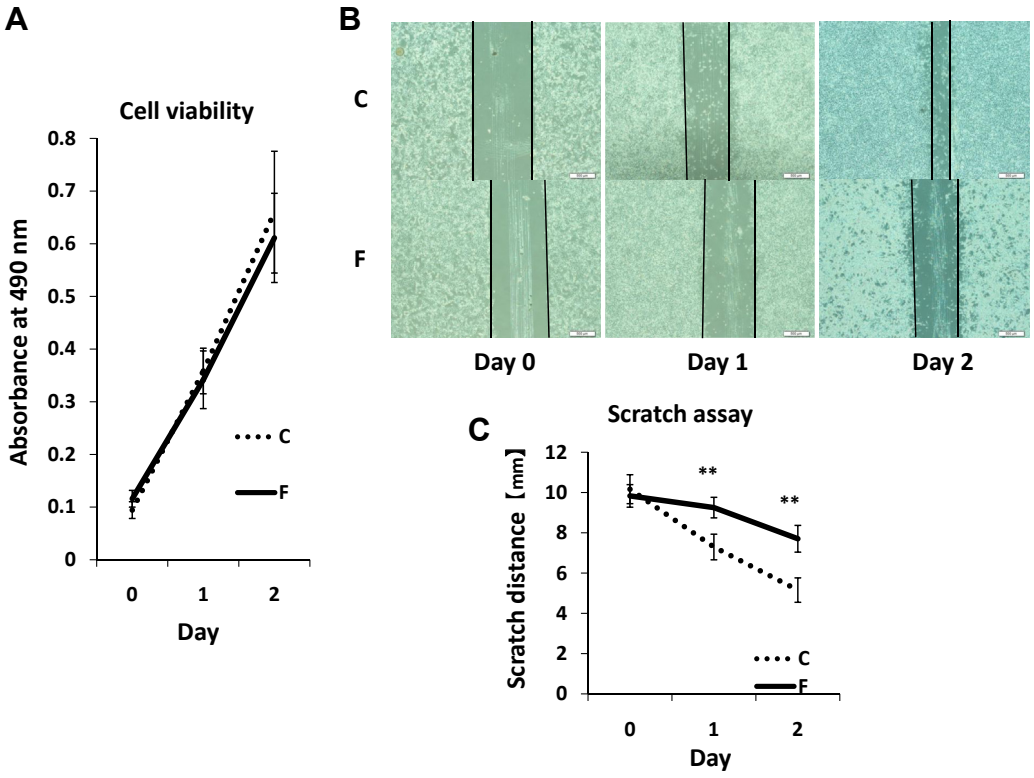

Fig 1. (*A*) Cell viability was measured with an MTT assay at 0, 24, and 48 hours after treatment. F group was treated with FUT-175 (80 μg/mL) and C group was vehicle only (distilled water). No difference was observed at any treatment time points between the F group and the C group. (*B*) Representative photographs of the scratch assay of "invasion" (×4 fields). (*C*) In the scratch assay, cell immigration across the scratched area was decreased in the F group compared with the C group ($P < .01$) at both 24 and 48 hours after treatment with FUT-175. $^{**}P < .01$. *MTT*, 3-(4,5-di-methylthiazol-2-yl)-2,5-diphenyltetrazolium bromide, yellow tetrazole; *FUT*, nafamostat mesilate.

[ICAM-1], anti−β-actin, VEGF [A-20], and MMP-14; 1:1,000 dilution) overnight, the membranes were then incubated with secondary antibody (1:10,000 dilution, Histofine; Nichirei, Tokyo, Japan). A luminol enhancer and the peroxide solution, Clarity Max (Bio-Rad Laboratories, Inc, Hercules, CA), were used to detect the protein bands with a ChemiDoc XRS+ system and Image Lab software (Bio-Rad).

Zymography

In addition to the MMP-2/9 expression levels, the activation levels of MMP-2/9 in the supernatant were analyzed with a gelatin zymography kit (Primary Cell, Hokkaido, Japan). PAN02 cells were treated for 24 hours with FUT-175 (80 μg/mL) as the F group or with vehicle alone (distilled water) as the C group. After treatment, the conditioned medium was concentrated 10-fold using Amicon Ultra-4 filter units (Merck, Darmstadt, Germany). Each sample was subjected to electrophoresis on a gelatin-containing gel. The gels were washed and incubated for 40 hours in an incubation buffer at 37°C. After Coomassie blue staining, the gels were scanned using a ChemiDoc XRS+ system and Image Lab software (Bio-Rad). The experimental procedure given earlier was conducted according to the manufacture's instructions and our previous study.[11,19]

MRI protocol

The animals were imaged in the prone position inside a clinical 9.4 T MRI system (Biospin 94/20 USR; Bruker, Ettingen, Germany) using a coronal, multislice, T2-weighted protocol (TurboRARE-T2) (Paravision 5.1; Bruker). Metastatic lesions were detected as a high signal area with a T2-weithted image. Although 9.4 T MRI can detect lesions <1 mm, however, in this study, liver metastases were defined as a long axis of >1 mm, which was not detected in previous studies or increased with time.

Statistical analysis

The experimental data are means ± standard deviations. The presence or absence of the differences were evaluated by the nonparametric Mann-Whitney *U* test with SPSS 23.0 (IBM Japan, Tokyo, Japan). DFS and overall survival (OS) were analyzed with GraphPad Prism, version 7.00 (GraphPad Software, San Diego, CA) using the Gehan-Breslow-Wilcoxon test.

Results

Cell proliferation and invasion assay

At 24 hours after treatment, there was no difference in cell proliferation between the C group and the F group (Fig 1, *A*). The "invasive ability" of the cells to move across the scratch was suppressed in the F group compared with the C group ($P < .01$) (Fig 1, *B* and *C*).

Suppression of NF-κB levels

The expression of IκBα was increased in the F group, and its phosphorylated counterpart (pIκBα) was decreased in the F group compared with the C group, most probably because FUT-175 stabilized IκBα and inhibited its phosphorylation.[20] Accordingly, the expression level of NF-κB was decreased in the F group compared with the C group (Fig 2, *A*).

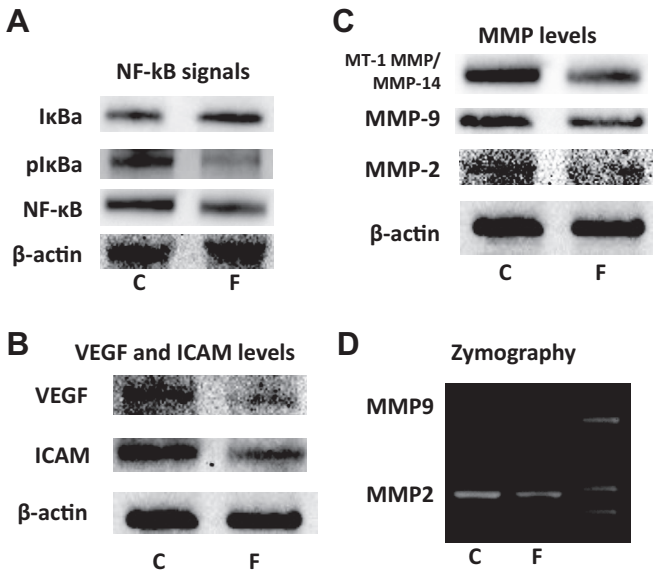

Fig 2. Western blotts in vitro. (*A*) The level of IκBα in the F group treated with FUT-175 was higher than that of the C group. In contrast, the level of phosphorylated-IκBα in the F group was lower than that of the C group. The level of NF-κB in the F group was lower than that of the C group. (*B*) The levels of MT-1 MMP/MMP-14 and MMP-2/9 were lower in the F group than in the C group. (*C*) The levels of VEGF and ICAM in the F group were lower than those in the C group. *D*. Zymography revealed lesser activity levels of both MMP-2/9 in the F group compared with the C group. *FUT*, nafamostat mesilate; *NF-κB*, nuclear factor-κb; *MT*, membrane type; *MMP*, matrix metalloproteinase; *VEGF*, vascular endothelial growth factor; *ICAM*, intracellular adhesion molecule.

Downregulation of NF-κB resulted in suppression of the expression of MMP-9, VEGF, and ICAM

As shown in Fig 2, *B* and *C*, the expression levels of VEGF, ICAM, and MMP-9 were suppressed in the F group compared with the C group, probably because ICAM and VEGF are downstream of NF-κB signal transduction and MMP-9 has an NF-κB—binding site in its activation site.

Downregulation of NF-κB activation leads to suppression of membrane type-1 MMP/MMP-14 and MMP-2 protein

NF-κB activates membrane type (MT)-MMP (MT-1 MMP/MMP-14), which causes the activation of pro-MMP-2. Our results showed a decrease of protein concentration in both MT-1 MMP/MMP-14 and MMP-2 in the F group compared with the C group (Figure 2, *C*).

Gelatin zymography

Zymography shows the activation levels of MMP-2/9 in the supernatant of the cell culture. The activity of both MMP-2 and MMP-9 was decreased in the F group compared with the C group (Fig 2, *D*). This result suggests that FUT-175 suppressed not only the protein levels but also the enzymatic activity levels of MMPs.

In vivo study

Representative data by MRI are shown in Fig 3, *A*. FUT-175 delayed tumor formation and hepatic metastasis. The expression levels of VEGF and ICAM were also decreased in the F group compared with the C group (Fig 3, *B*).

Treatment of cancer cells using FUT-175 before implantation improve both DFS and OS

The increases in both DFS and OS were statistically significant in the F group compared with the C group (Fig 4, *A* and *B*). In the C group, most of the recurrences were observed within a week; however, in the F group, median DFS was 3 weeks ($P < .05$) (95% confidence interval 1.249—7.208). OS in the C group was 5 weeks after the operation; OS in the F group was longer, with a median of 7 weeks ($P < .05$).

Systemic administration of FUT-175 inhibited the formation of liver metastasis

As shown in Fig 5, the average number of metastatic lesions was 2.4 for the C group and only 0.5 for the F group ($P < .01$), suggesting

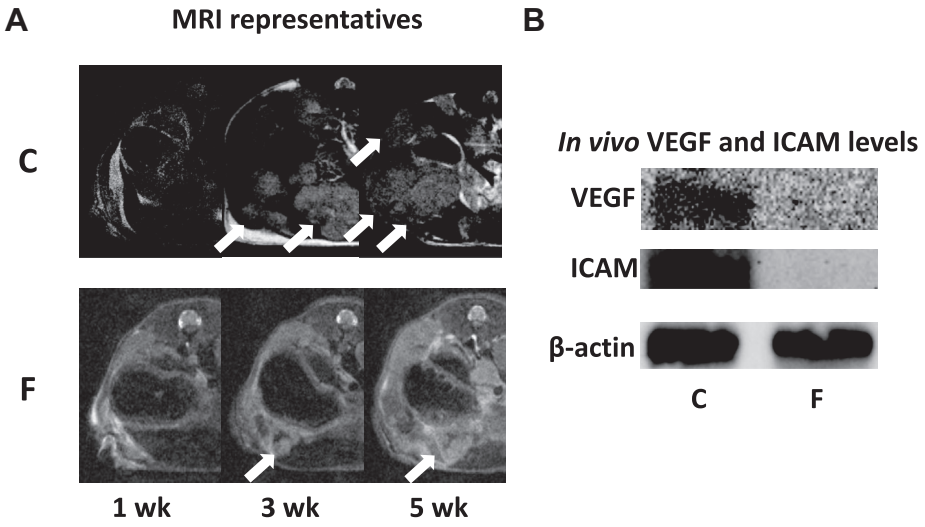

Fig 3. (*A*) Representative MRI images (T2 weighted) for both the C and the F groups. In the T2-weighted image, the tumor appears as a white mass (arrows). These MRI images show that the rate of liver metastases is less in the F group. (*B*) Western blotting from the excised liver tumor revealed the levels of VEGF and ICAM were lower in the F group. *MRI*, magnetic resonance imaging; *VEGF*, vascular endothelial growth factor; *ICAM*, intracellular adhesion molecule.

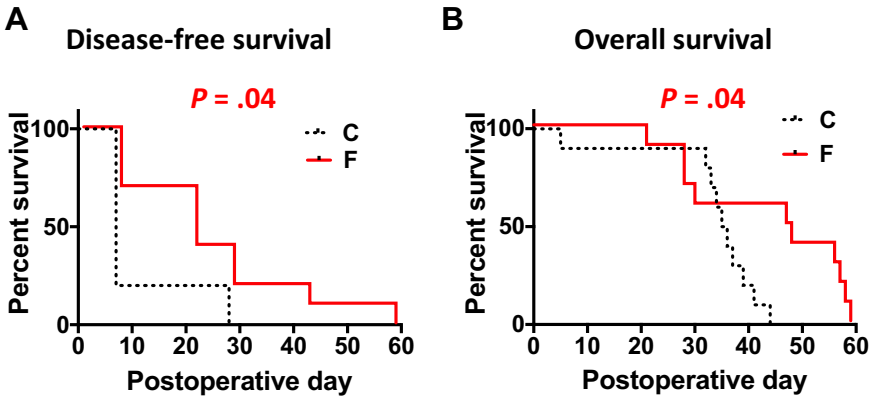

Fig 4. (*A*) DFS rates are compared between the C and the F groups. The time to development of a liver metastasis was greater in the F group ($P < .05$). (*B*) OS in the F group was also greater ($P < .05$). *DFS*, disease-free survival; *OS*, overall survival.

that systemic administration of FUT-175 also has the effect of decreasing the number of liver metastasis.

Discussion

FUT-175 is a broad-spectrum, serine protease inhibitor that directly suppresses serine type proteolytic enzymes.[21,22] One of the anti-inflammatory mechanisms of FUT-175 is known to inhibit NF-κB signaling.[23–25] We also have reported on NF-κB–related studies on improving anticancer, drug-induced chemo-resistance and inhibiting peritoneal dissemination in mice.[11,13,20,26]

Regarding NF-κB and invasion or metastasis, several studies have demonstrated the relationship between NF-κB and MMP-9.[27,28] The promoter region of the MMP-9 gene contains the binding site of NF-κB; therefore, MMP-9 expression decreases when NF-κB is suppressed.[29,30]

Also, some reports argue that NF-κB suppresses MMP-2 expression.[31–34] Few reports, however, focus on the molecular mechanisms between NF-κB and MMP-2.[35] MMP-2 expression is activated by pro-MMP-2, and pro-MMP-2 is activated by MT MMP/MT-1 MMP/MMP-14.[36–38] Furthermore, MT-1 MMP/MMP-14 expression is activated by NF-κB.[9] Therefore, MMP-2 and NF-κB have a relationship via MT-1 MMP/MMP-14.

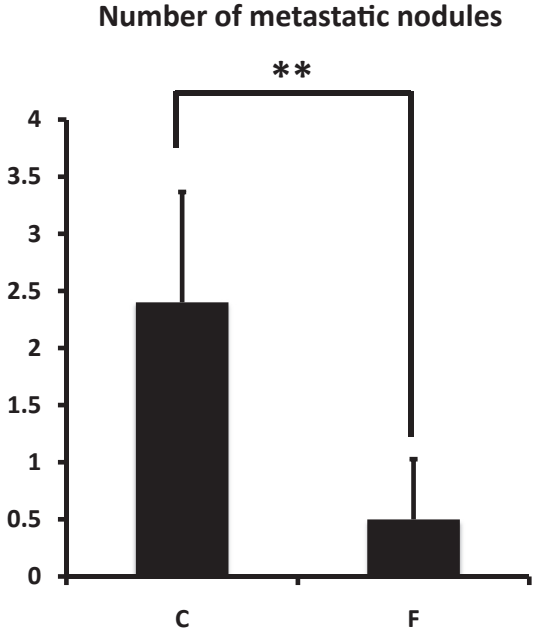

Fig 5. The number of metastatic foci in the group treated with FUT-175 is shown. The number of metastatic lesions was counted 7 days after operative inoculation of PAN02 cells. In the C group, the average number of metastasis nodules was 2.4, whereas in the F group, it was 0.5 ($P < .01$). $^{**}P < .01$. *FUT*, nafamostat mesilate.

MT-1 MMP/MMP-14 has been reported to activate MMP-2, a basement membrane–degrading enzyme, especially in cancer tissues.[36] MT-1 MMP/MMP-14 is overexpressed, especially in cancer cells, and MT-1 MMP/MMP-14 itself acts as a growth factor in malignant cancer cells, human breast carcinoma cells, human glioma cells, and hamster ovary cells.[39] Proliferation of cancer cells is suppressed when MT-1 MMP/MMP-14 activity was inhibited in pancreatic cancer, squamous carcinoma, and fibrosarcoma cells.[40] Recently, MT-1 MMP/MMP-14 in endothelial cell nuclei has been a target for cancer treatment because MT-1 MMP is key for tumor angiogenesis.[41]

Our study demonstrated that all the expression levels of NF-κB, MT-1 MMP/MMP-14, and MMP-2 were decreased by FUT-175. This finding suggests that in addition to suppression of MMP-9, FUT-175 suppressed both the expression and the activity of MMP-2, apparently via inhibition of the MT-1 MMP/MMP-14 pathway. Therefore, FUT-175 may act by suppressing both MMP-2 and MMP-9 activity, thereby helping to decrease liver metastasis in this murine model of pancreatic cancer metastases. To the best of our knowledge, this is the first report that has shown a close relationship of NF-κB, MT-1 MMP/MMP-14, and MMP-2 in association with FUT-175.

ICAM, which is a target gene of NF-κB, plays a crucial role in cell adhesion.[42] Furthermore, ICAM is also involved in the formation of cancer metastasis by helping circulating tumor cells adhere to endothelial cells.[43] Also, VEGF causes angiogenesis and plays an important role in the formation of metastases.[44] Once NF-κB expression is inhibited, the expressions of MMP-2/9, ICAM, and VEGF are suppressed, resulting in suppression of metastatic lesions.

The limitations of our current research are the route of administration and dose, which differ between mice and humans owing to differences in esterase activity. For clinical application, these problems would need to be solved. Nevertheless, FUT-175 is already in clinical use and has minimal adverse effects compared with the usual cytotoxic anticancer agents used for both unresectable pancreatic cancer and for adjuvant chemotherapy.[45] Introduction and standardization of early clinical trials are expected.

Funding/Support

This work was supported by Japan Society for the Promotion of Science (JSPS) KAKENHI Grant Number 19K18164.

Conflict of interest/Disclosure

The authors have indicated that they have no conflicts of interest regarding the content of this article.

References

1. Siegel RL, Miller KD, Jemal A. Cancer statistics, 2017. *CA Cancer J Clin*. 2017;67:7–30.
2. Chen Q, Boire A, Jin X, et al. Carcinoma-astrocyte gap junctions promote brain metastasis by cGAMP transfer. *Nature*. 2016;533:493–498.
3. Wu L, Luo Z, Zheng J, et al. IL-33 can promote the process of pulmonary fibrosis by inducing the imbalance between MMP-9 and TIMP-1. *Inflammation*. 2018;41:878–885.
4. Babykutty S, Priya PS, Nandini RJ, et al. Nimbolide retards tumor cell migration, invasion, and angiogenesis by downregulating MMP-2/9 expression via inhibiting ERK1/2 and reducing DNA-binding activity of NF-κB in colon cancer cells. *Mol Carcinog*. 2012;51:475–490.
5. Fakhrudin N, Waltenberger B, Cabaravdic M, et al. Identification of plumericin as a potent new inhibitor of the NF-κB pathway with anti-inflammatory activity in vitro and in vivo. *Br J Pharmacol*. 2014;171:1676–1686.
6. Huang H, Langenkamp E, Georganaki M, et al. VEGF suppresses T-lymphocyte infiltration in the tumor microenvironment through inhibition of NF-κB-induced endothelial activation. *FASEB J*. 2015;29:227–238.
7. Van Tubergen EA, Banerjee R, Liu M, et al. Inactivation or loss of TTP promotes invasion in head and neck cancer via transcript stabilization and secretion of MMP9, MMP2, and IL-6. *Clin Cancer Res*. 2013;19:1169–1179.
8. Shaverdashvili K, Wong P, Ma J, et al. MT1-MMP modulates melanoma cell dissemination and metastasis through activation of MMP2 and RAC1. *Pigment Cell Melanoma Res*. 2014;27:287–296.
9. Annabi B, Laflamme C, Sina A, Lachambre MP, Béliveau R. A MT1-MMP/NF-kappaB signaling axis as a checkpoint controller of COX-2 expression in CD133+ U87 glioblastoma cells. *J Neuroinflammation*. 2009;6:8.
10. Itoh Y, Takamura A, Ito N, et al. Homophilic complex formation of MT1-MMP facilitates proMMP-2 activation on the cell surface and promotes tumor cell invasion. *EMBO J*. 2001;20:4782–4793.
11. Fujiwara Y, Furukawa K, Haruki K, et al. Nafamostat mesilate can prevent adhesion, invasion and peritoneal dissemination of pancreatic cancer thorough nuclear factor kappa-B inhibition. *J Hepatobiliary Pancreat Sci*. 2011;18:731–739.
12. Furukawa K, Iida T, Shiba H, et al. Anti-tumor effect by inhibition of NF-kappaB activation using nafamostat mesilate for pancreatic cancer in a mouse model. *Oncol Rep*. 2010;24:843–850.
13. Horiuchi T, Uwagawa T, Shirai Y, et al. New treatment strategy with nuclear factor-kappaB inhibitor for pancreatic cancer. *J Surg Res*. 2016;206:1–8.
14. Ohno K, Nishimori H, Yasoshima T, et al. Inhibition of osteopontin reduces liver metastasis of human pancreatic cancer xenografts injected into the spleen in a mouse model. *Surg Today*. 2010;40:347–356.
15. Aoyama T, Ino Y, Ozeki M, et al. Pharmacological studies of FUT-175, nafamstat mesilate: I. inhibition of protease activity in in vitro and in vivo experiments. *Jpn J Pharmacol*. 1984;35:203–227.
16. Workman P, Aboagye EO, Balkwill F, et al. Guidelines for the welfare and use of animals in cancer research. *Br J Cancer*. 2010;102:1555–1577.
17. Paster EV, Villines KA, Hickman DL. Endpoints for mouse abdominal tumor models: Refinement of current criteria. *Comp Med*. 2009;59:234–241.
18. Shimada Y, Kobayashi H, Kawagoe S, et al. Endoplasmic reticulum stress induces autophagy through activation of p38 MAPK in fibroblasts from Pompe disease patients carrying c.546G>T mutation. *Mol Genet Metab*. 2011;104:566–573.
19. Sugano H, Shirai Y, Horiuchi T, et al. Nafamostat mesilate enhances the radiosensitivity and reduces the radiation-induced invasive ability of colorectal cancer cells. *Cancers (Basel)*. 2018;10.
20. Haruki K, Shiba H, Fujiwara Y, et al. Inhibition of nuclear factor-κB enhances the antitumor effect of paclitaxel against gastric cancer with peritoneal dissemination in mice. *Dig Dis Sci*. 2013;58:123–131.
21. Zhu J, Miao XR, Tao KM, et al. Trypsin-protease activated receptor-2 signaling contributes to pancreatic cancer pain. *Oncotarget*. 2017;8:61810–61823.
22. Li C, Wang J, Fang Y, et al. Nafamostat mesilate improves function recovery after stroke by inhibiting neuroinflammation in rats. *Brain Behav Immun*. 2016;56:230–245.
23. Shirai Y, Shiba H, Iwase R, et al. Dual inhibition of nuclear factor kappa-B and Mdm2 enhance the antitumor effect of radiation therapy for pancreatic cancer. *Cancer Lett*. 2016;370:177–184.
24. Uwagawa T, Yanaga K. Effect of NF-κB inhibition on chemoresistance in biliary-pancreatic cancer. *Surg Today*. 2015;45:1481–1488.
25. Furukawa K, Ohashi T, Haruki K, et al. Combination treatment using adenovirus vector-mediated tumor necrosis factor-alpha gene transfer and a NF-kappaB inhibitor for pancreatic cancer in mice. *Cancer Lett*. 2011;306:92–98.
26. Haruki K, Shiba H, Fujiwara Y, et al. Inhibition of nuclear factor-kappaB enhances the antitumor effect of tumor necrosis factor-alpha gene therapy for hepatocellular carcinoma in mice. *Surgery*. 2013;154:468–478.
27. Yeh CB, Hsieh MJ, Hsieh YH, Chien MH, Chiou HL, Yang SF. Correction: Anti-metastatic effects of norcantharidin on hepatocellular carcinoma by transcriptional inhibition of MMP-9 through modulation of NF-kB activity. *PLoS One*. 2017;12:e0171900.
28. Yan W, Fan W, Chen C, et al. IL-15 up-regulates the MMP-9 expression levels and induces inflammatory infiltration of macrophages in polymyositis through regulating the NF-kB pathway. *Gene*. 2016;591:137–147.
29. Bond M, Chase AJ, Baker AH, Newby AC. Inhibition of transcription factor NF-kappaB reduces matrix metalloproteinase-1, -3 and -9 production by vascular smooth muscle cells. *Cardiovasc Res*. 2001;50:556–565.
30. Bai XY, Li S, Wang M, et al. Krüppel-like factor 9 down-regulates matrix metalloproteinase 9 transcription and suppresses human breast cancer invasion. *Cancer Lett*. 2018;412:224–235.
31. Lu CY, Lai SC. Induction of matrix metalloproteinase-2 and -9 via Erk1/2-NF-κB pathway in human astroglia infected with Toxoplasma gondii. *Acta Trop*. 2013;127:14–20.
32. Chen YY, Lu HF, Hsu SC, et al. Bufalin inhibits migration and invasion in human hepatocellular carcinoma SK-Hep1 cells through the inhibitions of NF-kB and matrix metalloproteinase-2/-9-signaling pathways. *Environ Toxicol*. 2015;30:74–82.
33. Huang M, Xin W. Matrine inhibiting pancreatic cells epithelial-mesenchymal transition and invasion through ROS/NF-kappaB/MMPs pathway. *Life Sci*. 2018;192:55–61.
34. Jia XJ, Li X, Wang F, Liu HQ, Zhang DJ, Chen Y. Berbamine exerts anti-inflammatory effects via inhibition of NF-κB and MAPK signaling pathways. *Cell Physiol Biochem*. 2017;41:2307–2318.
35. Yang XC, Wang X, Luo L, et al. RNA interference suppression of A100A4 reduces the growth and metastatic phenotype of human renal cancer cells via NF-kB-dependent MMP-2 and bcl-2 pathway. *Eur Rev Med Pharmacol Sci*. 2013;17:1669–1680.
36. Sato H, Takino T, Okada Y, et al. A matrix metalloproteinase expressed on the surface of invasive tumour cells. *Nature*. 1994;370:61–65.
37. Park JM, Kim A, Oh JH, Chung AS. Methylseleninic acid inhibits PMA-stimulated pro-MMP-2 activation mediated by MT1-MMP expression and further tumor invasion through suppression of NF-kappaB activation. *Carcinogenesis*. 2007;28:837–847.
38. Sato H, Takino T. Coordinate action of membrane-type matrix metalloproteinase-1 (MT1-MMP) and MMP-2 enhances pericellular proteolysis and invasion. *Cancer Sci*. 2010;101:843–847.
39. Remacle AG, Rozanov DV, Baciu PC, Chekanov AV, Golubkov VS, Strongin AY. The transmembrane domain is essential for the microtubular trafficking of membrane type-1 matrix metalloproteinase (MT1-MMP). *J Cell Sci*. 2005;118:4975–4984.
40. Hotary KB, Allen ED, Brooks PC, Datta NS, Long MW, Weiss SJ. Membrane type I matrix metalloproteinase usurps tumor growth control imposed by the three-dimensional extracellular matrix. *Cell*. 2003;114:33–45.
41. Barillari G, Iovane A, Bacigalupo I, et al. The HIV protease inhibitor indinavir down-regulates the expression of the pro-angiogenic MT1-MMP by human endothelial cells. *Angiogenesis*. 2014;17:831–838.
42. Zhu S, Xu X, Liu K, Gu Q, Wei F, Jin H. Peptide GC31 inhibits chemokines and ICAM-1 expression in corneal fibroblasts exposed to LPS or poly(I:C) by blocking the NF-κB and MAPK pathways. *Exp Eye Res*. 2017;164:109–117.
43. Lian S, Lu Y, Cheng Y, et al. S-nitrosocaptopril interrupts adhesion of cancer cells to vascular endothelium by suppressing cell adhesion molecules via inhibition of the NF-κB, CyrillicB and JAK/STAT signal pathways in endothelial cells. *Eur J Pharmacol*. 2016;791:62–71.
44. Sanders AJ, Ye L, Mason MD, Jiang WG. The impact of EPLINα (epithelial protein lost in neoplasm) on endothelial cells, angiogenesis and tumorigenesis. *Angiogenesis*. 2010;13:317–326.
45. Uwagawa T, Misawa T, Tsutsui N, et al. Phase II study of gemcitabine in combination with regional arterial infusion of nafamostat mesilate for advanced pancreatic cancer. *Am J Clin Oncol*. 2013;36:44–48.